molecular pharmaceutics

Article

pubs.acs.org/molecularpharmaceutics

Synthesis of Doxorubicin α-Linolenic Acid Conjugate and Evaluation of Its Antitumor Activity

Chun-hui Liang,[†,§,∥] Wei-liang Ye,[†,∥] Chun-lai Zhu,[†] Ren Na,[†] Ying Cheng,[†] Han Cui,[†] Dao-zhou Liu,[†] Zhi-fu Yang,*[,‡] and Si-yuan Zhou*[,†]

[†]Department of Pharmaceutics, School of Pharmacy, Fourth Military Medical University, Xi'an 710032, China

[‡]Department of Pharmacy, Xijing Hospital, Fourth Military Medical University, Xi'an 710032, China

[§]Department of Pharmacy, Xi'an Children's Hospital, Xi'an 710002, China

Supporting Information

ABSTRACT: Doxorubicin (DOX) is a broad-spectrum antitumor drug used in the clinic. However, it can cause serious heart toxicity. To increase the therapeutic index of DOX and to attenuate its toxicity toward normal tissues, we conjugated DOX with either α-linolenic acid (LNA) or palmitic acid (PA) by a hydrazone or an amide bond to produce DOX-hyd-LNA, DOX-ami-LNA, DOX-hyd-PA, and DOX-ami-PA. The cytotoxicity of DOX-hyd-LNA on HepG2, MCF-7, and MDA-231 cells was higher compared to that of DOX, DOX-ami-LNA, DOX-hyd-PA, and DOX-ami-PA. The cytotoxicity of DOX-hyd-LNA on HUVECs was lower than that of DOX. DOX-hyd-LNA released significantly more DOX in pH 5.0 medium than it did in pH 7.4 medium. DOX-hyd-LNA induced more apoptosis in MCF-7 and HepG2 cells than DOX or DOX-ami-LNA. Significantly more DOX was released from DOX-hyd-LNA in both MCF-7 and HepG2 cells compared with DOX-ami-LNA. Compared to free DOX, a biodistribution study showed that DOX-hyd-LNA greatly increased the content of DOX in tumor tissue and decreased the content of DOX in heart tissue after it was intravenously administered. DOX-hyd-LNA improved the survival rate, prolonged the life span, and slowed the growth of the tumor in tumor-bearing nude mice. These results indicate that DOX-hyd-LNA improved the therapeutic index of DOX. Therefore, DOX-hyd-LNA is a potential compound for use as a cancer-targeting therapy.

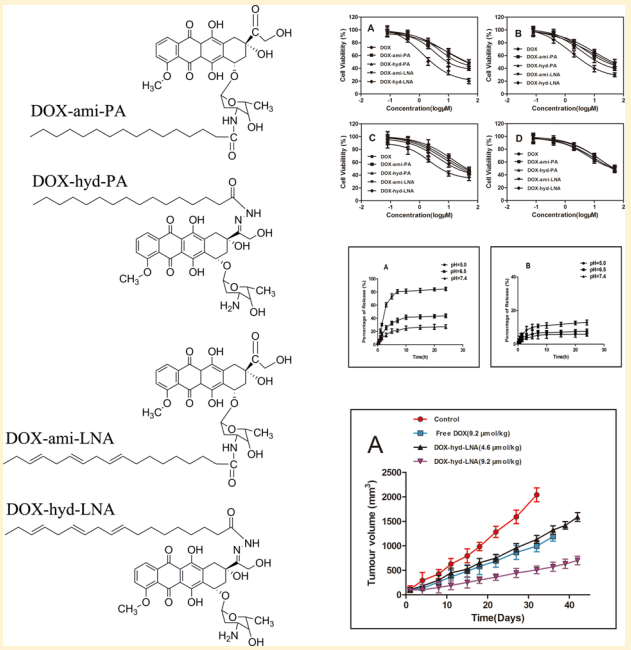

KEYWORDS: *doxorubicin, α-linolenic acid, palmitic acid, pH sensitive, tumor targeting*

1. INTRODUCTION

Doxorubicin (DOX) is an important antitumor drug that is used in the clinic, but it can cause serious adverse effects, such as cardiomyopathy and congestive heart failure.[1−4] Many methods have been explored to increase the therapeutic index of DOX, including its use with nanoparticles, liposomes, and dendrimers.[5−10] Additionally, a prodrug strategy has also been extensively investigated to selectively improve the interaction between the drug and the cells that it targets.[11,12]

To design a tumor-targeting drug, it is crucial to understand the tumor cell microenvironment. Tumor cells are different from normal cells, as they grow quickly and usually require a large amount of various nutrients. Therefore, tumor cells highly express receptors, such as the folate receptor and transferrin receptor, to facilitate the uptake of nutrients. The folate receptor has been used as a target to mediate the uptake of antitumor drugs by tumor cells.[13−15]

Polyunsaturated fatty acids (PUFAs) are essential fatty acids for human health. Human beings can obtain PUFAs only from the diet. There are 18−22 carbons and 2−6 unsaturated carbon−carbon double bonds in a PUFA molecule. PUFAs have shown significant cytotoxicity toward CFPAC, PANC-1, and HL-60 leukemia cells, and their in vivo antitumor activities have been studied with animals and humans.[16−21] In addition, compared with normal cells, PUFAs are more avidly taken up by tumor cells.[22−24] Thus, PUFAs have been used as tumor-

Received: July 17, 2013
Revised: March 21, 2014
Accepted: March 31, 2014
Published: March 31, 2014

specific ligands to guide antitumor drugs to recognize tumor cells selectively.[25,26] Taxoprexin was synthesized by connecting docosahexaenoic acid (DHA, a PUFA) with paclitaxel through an ester bond. Compared with paclitaxel, taxoprexin greatly enhanced the therapeutic index and decreased the systemic toxicity of paclitaxel.[27] Taxoprexin has entered phase III clinical trials.[27]

The promising antitumor activity of taxoprexin has prompted more extensive investigation of different PUFA−taxoid conjugates. Ojima et al. connected second-generation taxoids, SB-T-1213, with DHA, LNA, and linoleic acid (LA), and their antitumor activity was evaluated in a drug-resistant (P-glycoprotein positive) DLD-1 tumor xenograft model. LNA-SB-T-1213 showed higher antitumor activity than DHA-SB-T-1213 when given at the same dose. Thus, the antitumor activity of DHA-SB-T-1213 was greater than LA-SB-T-1213. Paclitaxel, however, was ineffective. These results implied that LNA could be utilized for PUFA−antitumor drug conjugates in addition to DHA.[25] Accordingly, Wang et al. conjugated DOX with DHA through a hydrazone bond, and an in vivo experiment indicated that compared with free DOX the therapeutic effect of DHA-DOX was obviously increased in tumor-bearing mice.[28] Thereafter, a series of DOX derivatives were synthesized by connecting doxorubicin-14-hemisuccinate with different substituent groups, and their cytotoxicity was determined by MTT assays. The results indicated that the *N*-tetradecyl amide derivative showed the greatest cytotoxicity toward tumor cells of all of the derivatives, and its antitumor activity in vitro was almost the same as free DOX.[29] Furthermore, by using unsaturated and saturated fatty acid, a series of *N*-acyl hydrazone derivatives of DOX (including DOX-hyd-LNA) were synthesized, and their cytotoxicity was evaluated by MTT assay. The results indicated that *N*-acyl hydrazone derivatives had some merits with regard to their cytotoxicity and ability to avoid multidrug resistance.[30] Although fatty acid derivatives of DOX have been studied, a deeper and more systematic study on DOX−fatty acyl conjugates is necessary.

In our previous studies, we conjugated DOX with α-linolenic acid through an amide bond to improve the uptake of DOX in cancer cells.[31] To study the potential use of LNA in DOX delivery systems further, we conjugated DOX with LNA or palmitic acid (PA, a saturated fatty acid) by either a hydrazone or an amide bond, and their drug-release characteristics and antitumor activity were investigated in vitro and in vivo.

2. MATERIALS AND METHODS

2.1. Materials. Doxorubicin·HCl (DOX·HCl) was purchased from Hisun Pharmaceutical Co. (Zhejiang province, China). α-Linolenic acid (LNA), palmitic acid (PA), 3-(4,5-dimethylthiazol-2-yl)-2,5-diphenyl tetrazolium bromide (MTT), 1-ethyl-(3-(dimethylamino)propyl)-carbodiimide (EDCI), and *N*-hydroxysuccinimide (NHS) were purchased from Sigma-Aldrich (St. Louis, MO). Athymic nude mice (female, body weight 20−23 g) were purchased from the Experimental Animal Center of the Fourth Military Medical University. Mice were fed in a pathogen-free environment with a 12 h light/dark cycle and were freely supplied with water and food throughout the experiments. All experiments using mice were carried out according to protocols that were approved by the Animal Care and Use Committee of the Fourth Military Medical University (authorized date: 17/03/2012, no. 12027).

2.2. Methods. *2.2.1. Synthesis of DOX-hyd-LNA.* The synthetic route of DOX-hyd-LNA is shown in Figure 1.

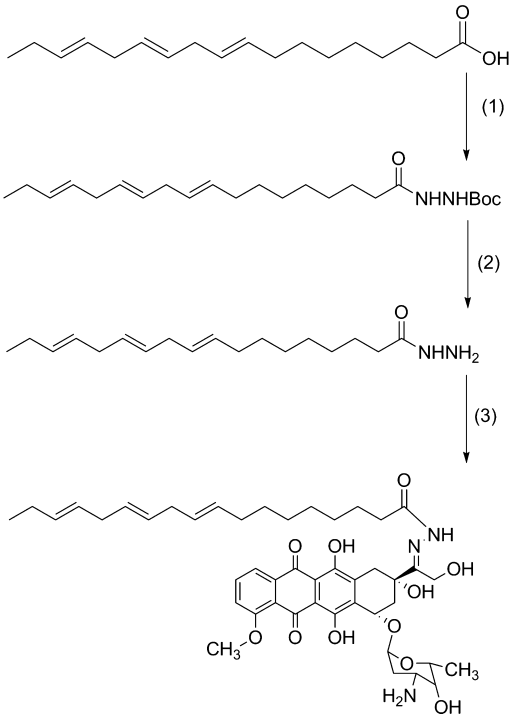

Figure 1. Reaction route for the synthesis of DOX-hyd-LNA: (1) $H_2NNHBoc$, EDCI, DMF; (2) TFA, CH_2Cl_2; (3) DOX, TFA, CH_2Cl_2.

2.2.1.1. Synthesis of N-Boc-LNA Hydrazine. To synthesize N-Boc-LNA hydrazine, 278 mg of LNA (1 mmol), 9 mL of dimethylformamide (DMF), 158.4 mg of $H_2NNHBoc$ (1.2 mmol), and 573 mg of EDCI (3 mmol) were added to a flask, and the mixture was stirred at 25 °C for 12 h. Water (10 mL) was added into the reaction mixture, which was then extracted with ethyl acetate. The organic phase was dried with Na_2SO_4 and evaporated using a vacuum rotary evaporator. N-Boc-LNA hydrazine was purified via a silica gel column using ethyl acetate/cyclohexane (v/v 2:1, R_f = 0.46) as the eluant. The compound was a pale yellow oily liquid. The yield was 372.2 mg (0.95 mmol, 85.3%). The mass spectrum and ^{1}H NMR spectrum of N-Boc-LNA hydrazine are shown in Supporting Information Figure 1. The molecular ion peak ($[M - H]^-$) of N-Boc-LNA hydrazine was 391. The ^{1}H NMR spectrum of N-Boc-LNA hydrazine exhibited typical signals at chemical shifts of δ 5.28−5.40 (6H, m), 2.81 (4H, s), 2.02−2.10 (4H, m), 1.64−1.66 (2H, m), 1.47 (9H, s, Boc), 1.31−1.39 (10H, m), 0.98 (3H, t, CH_3, J = 7.4 Hz) ppm.

2.2.1.2. Synthesis of LNA Hydrazine. To synthesize of LNA hydrazine, 274.4 mg of N-Boc-LNA hydrazine (0.7 mmol) was dissolved in 18 mL of dichloromethane and 6 mL of trifluoroacetic acid (TFA). The mixture was stirred at 25 °C for 15 min, the pH of the reaction mixture was then adjusted to 7 using 10% $NaHCO_3$, and 80 mL of dichloromethane was added. The organic phase was isolated and washed with 80 mL of water two times. The organic phase was dried with Na_2SO_4 and evaporated using a vacuum rotary evaporator. LNA hydrazine was purified via a silica gel column using dichloromethane/methanol (v/v 30:1, R_f = 0.29) as the eluant. The compound was a deep yellow oily liquid. The yield was 219.9 mg (0.75 mmol, 80.2%). The mass spectrum and ^{1}H NMR spectrum of LNA-$NHNH_2$ are shown in Supporting Information Figure 2. The molecular ion peak ($[M + H]^+$) of

dx.doi.org/10.1021/mp4004139 | *Mol. Pharmaceutics* 2014, 11, 1378−1390

LNA-$NHNH_2$ was 293. The ^1H NMR spectrum of LNA-$NHNH_2$ exhibited typical signals at chemical shifts of δ 5.28−5.43 (6H, m), 2.81 (4H, s), 2.03−2.10 (4H, m), 1.63 (2H, s), 1.24−1.31 (10H, m), 0.97 (3H, t, CH_3, J = 7.6 Hz) ppm.

2.2.1.3. Synthesis of the DOX-hyd-LNA Conjugate. To synthesize the DOX-hyd-LNA conjugate, 70.6 mg of DOX (0.13 mmol), 52.9 mg of LNA-hydrazine (0.18 mmol), 25 mL of dichloromethane, and 12 μL of TFA were added to a flask, the mixture was stirred overnight at 25 °C, and the organic phase was evaporated in the darkness. Then, DOX-hyd-LNA was purified via a silica gel column using dichloromethane/methanol (v/v 5:1, R_f = 0.86) as the eluant. The product was dried in a vacuum drying chamber. DOX-hyd-LNA was a dark red solid. The yield was 61.1 mg (0.075 mmol, 49.4%). The mass spectrum and ^1H NMR spectrum of DOX-hyd-LNA are shown in Supporting Information Figure 3. The molecular ion peak ($[M + H]^+$) of DOX-hyd-LNA was 819. The ^1H NMR spectrum of DOX-hyd-LNA exhibited typical signals at chemical shifts of 5.12−5.60 (9H, m), 3.82−4.21 (7H, m), 3.30−3.53 (3H, m), 2.60−2.78 (6H, m), 2.41−2.58 (5H, m), 1.97−2.06 (5H, m), 1.66−1.90 (3H, m), 1.14−1.66 (14H, m), 0.92 (3H, t, CH_3, J = 6.8 Hz) ppm.

The purification of DOX-hyd-LNA (dissolved in DMSO) was analyzed by a Waters HPLC equipped with a 2996 PDA detector and 2695 pump (Waters Corporation, USA). A Waters Symmetry C_{18} column (4.6 × 250 mm, 5 μm) was used as the analytical column, 70% acetonitrile and 30% H_2O were used as the mobile phase, and the flow rate was 1 mL/min. The wavelength of the PDA detector was 230 nm, and the analytical volume was 20 μL. The column temperature was kept at 25 °C.

Partition coefficients (Log P) of DOX·HCl, DOX, and DOX-hyd-LNA were measured using the *n*-octanol/water method.[29] The compound concentration in the two phases was detected by a UV−vis spectrophotometer (Beckman DU-800, USA).

2.2.2. Synthesis of DOX-ami-LNA. The synthetic route of DOX-ami-LNA is shown in Figure 2: 250 mg of LNA (0.89 mmol), 138 mg of NHS (1.2 mmol), 573 mg of EDCI (3 mmol), 120 μL of triethyl amine (TEA), 234.8 mg of DOX (0.43 mmol), and 25 mL of dichloromethane were added to a flask, and the mixture was stirred for 12 h at 25 °C. After that, the organic phase was evaporated, and the residue was purified using a silica gel column. The product was dried in a vacuum drying chamber. The yield was 350.5 mg (0.44 mmol, 72.4%).

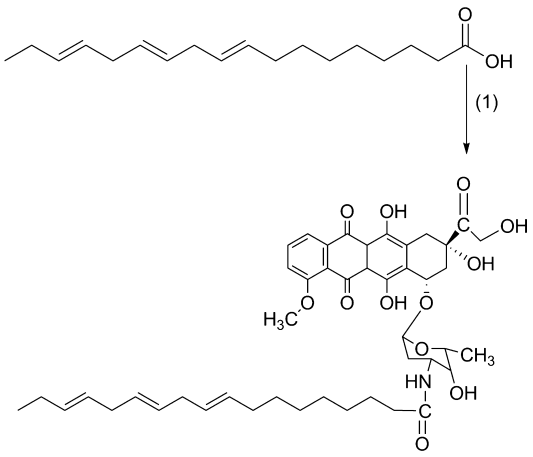

Figure 2. Reaction route for the synthesis of DOX-ami-LNA: (1) DOX, NHS, EDCI, TEA, CH_2Cl_2.

The purity and Log P of DOX-ami-LNA were determined as described above. The mass spectrum and ^1H NMR spectrum of DOX-ami-LNA have been published previously.[31]

2.2.3. Synthesis of DOX-hyd-PA and DOX-ami-PA. The synthetic routes of DOX-hyd-PA and DOX-ami-PA are shown in Figures 3 and 4, respectively. The synthetic methods for DOX-hyd-PA and DOX-ami-PA were as the same as those of DOX-hyd-LNA and DOX-ami-LNA. The compounds were dried in a vacuum drying chamber. The yields of DOX-hyd-PA and DOX-ami-PA were 52.4 and 72.4%, respectively. The purity and Log P of the compounds were detected as described above.

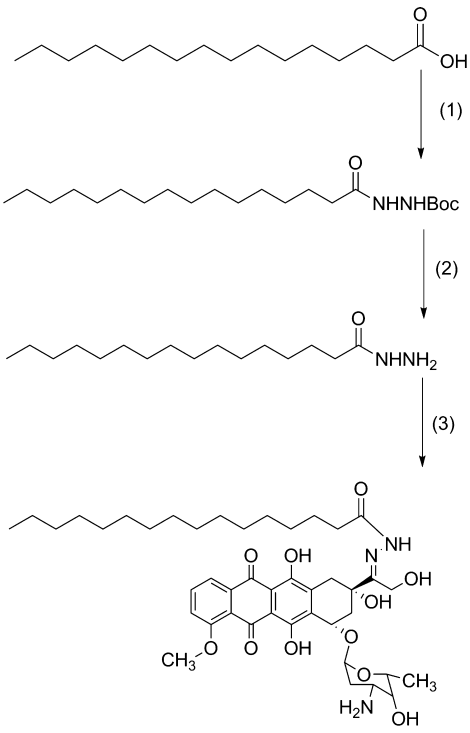

Figure 3. Reaction route for the synthesis of DOX-hyd-PA: (1) $H_2NNHBoc$, EDCI, DMF; (2) TFA, CH_2Cl_2; (3) DOX, TFA, CH_2Cl_2.

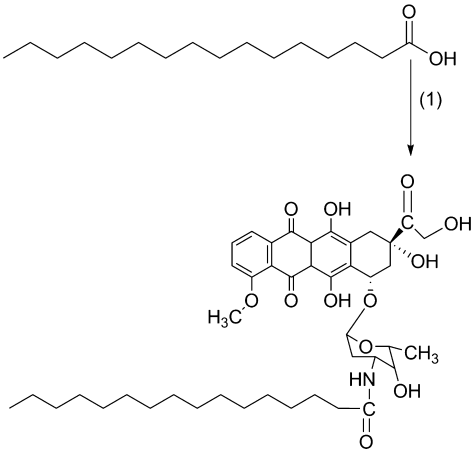

Figure 4. Reaction route for the synthesis of DOX-ami-PA: (1) DOX, NHS, EDCI, TEA, CH_2Cl_2.

The mass spectrum and ^1H NMR spectrum of PA-$NHNH_2$, DOX-hyd-PA, and DOX-ami-PA are shown in Supporting

dx.doi.org/10.1021/mp4004139 | *Mol. Pharmaceutics* 2014, 11, 1378−1390

Table 1. Mass Spectrum Conditions

compound	precursor	daughter	dwell time (s)	capillary voltage (kV)	cone voltage (V)	collision energy (eV)
DOX-hyd-LNA	817	690	0.2	2.5	55	18
DOX-ami-LNA	803	416	0.2	2.5	48	22
DOX	542	395	0.2	2.5	40	16

Information Figures 4−6, respectively. The molecular ion peak ($[M + H]^+$) of PA-$NHNH_2$ was 271. The ^1H NMR spectrum of PA-$NHNH_2$ exhibited typical signals at chemical shifts δ 6.65 (1H, s), 2.12−2.16 (2H, d,), 1.61−1.65 (3H, t), 1.25−1.28 (31H, m), 0.86−0.89 (3H, t, CH_3) ppm. The molecular ion peak ($[M + H]^+$) of DOX-hyd-PA was 797. The ^1H NMR spectrum of DOX-hyd-PA exhibited typical signals at chemical shifts of δ 10.01 (1H, s), 8.03 (1H, s), 7.78 (1H, s), 5.53−5.52 (2H, d), 4.68 (2H, d), 3.91−4.09 (3H, m), 3.08−3.46 (6H, m), 2.03−2.60 (7H, m), 1.67−1.98 (8H, m), 1.02−1.42 (29H, m), 0.85−0.88 (6H, m) ppm. The molecular ion peak ($[M - H]^-$) of DOX-ami-PA was 781. The ^1H NMR spectrum of DOX-ami-PA exhibited typical signals at chemical shifts of δ 13.97 (1H, s), 13.23 (1H, s), 7.78−8.04 (1H, s), 7.26−7.39 (1H, s), 7.26 (1H, s), 5.79−5.81 (1H, s), 5.45−5.55 (1H, s), 5.20−5.32 (2H, d), 4.68−4.83 (2H, d), 4.53−4.58 (1H, s), 3.96−4.28 (5H, m) 3.56−3.66 (1H, s), 2.97−3.02 (2H, d), 1.48−2.52 (14H, m), 1.01−1.42 (34H, m), 0.79−0.96 (4H, m) ppm.

2.2.4. Cell Culture. HUVECs are human umbilical vein endothelial cells.[32−34] MDA-MB-231 cells are a human breast cancer cell line that does not express the estrogen receptor.[35,36] MCF-7 cells are a human breast cancer cell line that expresses the estrogen receptor normally.[36,37] HepG2 cells are a human hepatoblastoma cell line.[38,39] All cell lines were obtained from the Institute of Biochemistry and Cell Biology, Chinese Academy of Sciences, Shanghai, China. All cells were cultured in RPMI 1640 medium containing penicillin (100 units/mL), streptomycin (100 μg/mL), and fetal bovine serum (10%).

2.2.5. Cytotoxicity of DOX Conjugates. The cytotoxicity of DOX-hyd-LNA, DOX-ami-LNA, DOX-hyd-PA, and DOX-ami-PA was evaluated by MTT assay. All compounds were dissolved in cell culture medium containing 5% (v/v) poly(ethylene glycol) 400 (PEG400). The cells were grown in 96-well plates at a density of 1×10^4 cells/well and incubated for 12 h. The medium was discarded, fresh drug-containing medium was added, and cells were incubated for 48 h. The wells were gently rinsed three times with PBS, fresh medium containing 5 mg/mL of MTT was added, and cells were incubated for 4 h. After that, the medium was discarded, and 150 μL of DMSO was added. Lastly, the plate was gently rocked for 10 min. The absorbance was detected at 570 nm by a Bio-Rad microplate reader. The cell culture experiments were performed in quintuplicate.

2.2.6. Stability of DOX-hyd-LNA and DOX-ami-LNA in Rat Serum. DOX-hyd-LNA (2 mg dissolved in 2 mL of normal saline containing 5% (v/v) PEG400) or DOX-ami-LNA (2 mg dissolved in 2 mL of normal saline containing 5% (v/v) PEG400) was added into 20 mL of fresh rat serum, and the mixture was cultured in a water bath shaker at 37 °C. Then, 50 μL of the incubated sample was taken out at predetermined time intervals, and the same volume of fresh serum was supplemented into the original mixture. One-hundred microliters of acetonitrile was added into the 50 μL drug-containing serum sample. The mixture was vigorously shaken and centrifuged at 8000*g*. The supernatant was collected and analyzed by HPLC−MS/MS.

2.2.7. DOX Release from DOX-hyd-LNA and DOX-ami-LNA in Medium with Different pH Values. To investigate the DOX-release characteristics of DOX-hyd-LNA and DOX-ami-LNA in vitro, sodium phosphate buffer (pH 7.4) and sodium acetate buffer (pH 5.0 and 6.5) were used as the release media. DOX-hyd-LNA (2 mg dissolved in 2 mL of water containing 5% (v/v) PEG400) or DOX-ami-LNA (2 mg dissolved in 2 mL of water containing 5% (v/v) PEG400) was added into 20 mL of release medium and cultured in a water bath shaker at 37 °C. Then, 50 μL of the incubated sample was taken out at predetermined time intervals, and the same volume of fresh medium was supplemented into the original mixture. The 20 μL sample was analyzed by HPLC−MS/MS.

2.2.8. HPLC−MS/MS Conditions. A Waters Quattro Premier LC−MS/MS system (Milford, MA, USA) and MassLynx 4.1 software was used. Briefly, a Waters XTerra C_{18} column (150 × 2.1 mm, 5 μm) was used as the analytical column, 80% acetonitrile and 20% H_2O were used as the mobile phase, and the flow rate was 0.2 mL/min. Multiple reaction monitoring operated in the negative ion mode was used. The source temperature and the desolvation temperature were set at 110 and 300 °C, respectively. The desolvation and cone gases were nitrogen, and its flow rates were 650 and 50 L/h, respectively. The collision gas was argon, and its flow rate was 0.18 mL/min. The analytical volume was 20 μL. The mass spectrum conditions to detect DOX, DOX-ami-LNA, and DOX-hyd-LNA are shown in Table 1. Under the optimized chromatographic conditions, DOX, DOX-ami-LNA, DOX-hyd-LNA, and any interference were completely separated. The linear range of the analytical method was 0.4−300 ng/mL, and the correlation coefficient was 0.9986.

2.2.9. Apoptosis Analysis. HepG2 cells (or MCF-7 cells) were grown into 6-well plates at density of 5×10^6 cells/mL for 24 h. Free DOX, DOX-ami-LNA, or DOX-hyd-LNA (dissolved in cell culture medium containing 5% (v/v) PEG400) was added, and cells were incubated for 24 h. The medium was discarded, and the cells were gently rinsed three times with PBS. Then, the cells were collected in PBS and centrifuged at 1000*g* for 2 min. After the supernatant was removed, the cells were resuspended in 0.2 mL of PBS. Lastly, after the cells were stained with annexin V−FITC and propidium iodide, they were analyzed with a Becton Dickinson FACScan cytometer.

2.2.10. Uptake of DOX-hyd-LNA and DOX-ami-LNA in Tumor Cells. HepG2 and MCF-7 cells were grown in 6-well plates at a density of 1×10^5 cells/mL. After 12 h, the medium was discarded, and DOX-hyd-LNA or DOX-ami-LNA (dissolved in cell culture medium containing 5% (v/v) PEG400) was added. After the cells were cultured for 30 or 120 min, the medium was discarded, and the cells were gently rinsed with PBS three times. Then, cells were collected in 1 mL of deionized water. The cell lysate was obtained by freezing and thawing the cells three times. The cell lysate was centrifuged at 8000*g*, and the supernatant was analyzed by HPLC−-MS/MS.

dx.doi.org/10.1021/mp4004139 | *Mol. Pharmaceutics* 2014, 11, 1378−1390

Table 2. Molecular Properties of DOX Conjugates (n = 5)

compound	Log P	molecular weight	number of oxygens and nitrogens atom	number of -OH and -NH	violations of rule of five	number of rotatable bonds
DOX·HCl	−1.45 ± 0.22	580.0	12	6	3	5
DOX	0.33 ± 0.08	543.5	12	6	3	5
DOX-ami-PA	0.87 ± 0.12	781.9	13	5	3	22
DOX-hyd-PA	0.93 ± 0.11	796.1	14	6	3	22
DOX-ami-LNA	1.09 ± 0.16	803.9	13	5	3	21
DOX-hyd-LNA	1.17 ± 0.18	818.1	14	6	3	21

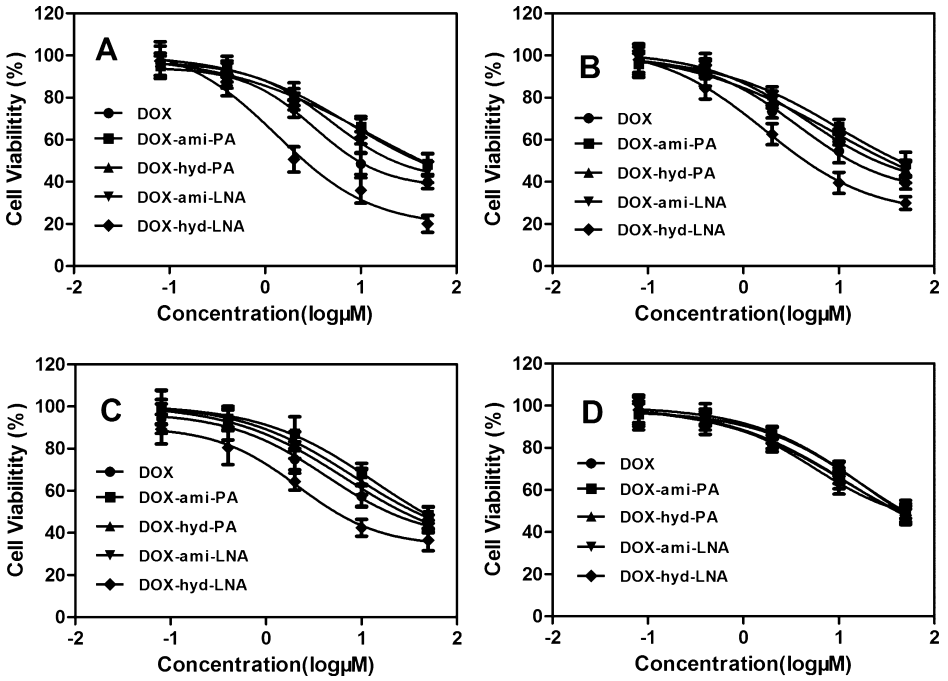

Figure 5. Cytotoxicity of DOX, DOX-hyd-LNA, DOX-ami-LNA, DOX-hyd-PA, and DOX-ami-PA against the following cells: HepG2 (A), MCF-7 (B), MDA-MB-231 (C), and HUVEC (D). Cells were incubated with DOX, DOX-hyd-LNA, DOX-ami-LNA, DOX-hyd-PA, and DOX-ami-PA for 48 h. n = 5.

Table 3. IC_{50} of DOX Conjugates on MCF-7, MDA-MB-231, HepG2, and HUVEC Cells

	IC_{50} (μM)			
compound	HepG2	MCF-7	MDA-MB-231	HUVEC
DOX	3.2 ± 0.7	3.6 ± 1.3	4.3 ± 1.1	5.5 ± 1.8
DOX-ami-PA	12.3 ± 1.4	9.8 ± 2.6	13.5 ± 2.2	16.9 ± 3.4
DOX-hyd-PA	7.8 ± 1.9	8.8 ± 1.8	8.1 ± 1.3	11.1 ± 2.6
DOX-ami-LNA	4.9 ± 0.8	4.6 ± 1.5	6.6 ± 1.7	19.0 ± 4.9
DOX-hyd-LNA	1.3 ± 0.4^{a,b,c}	1.7 ± 0.3^{a,b,c}	2.2 ± 0.7^{a,b,c}	12.1 ± 3.5^{a}

$^{a}p < 0.05$ vs DOX. $^{b}p < 0.01$ vs DOX-ami-LNA. $^{c}p < 0.01$ vs DOX-hyd-PA; n = 5.

The protein content in the cell lysates was determined by the Bradford method, and the drug content was normalized by the protein content of the cell lysate. The cell culture experiments were performed in quintuplicate.

2.2.11. Animal Experiments. 2.2.11.1. Maximum Tolerated Dose (MTD) Studies. DOX or DOX-hyd-LNA was dissolved in normal saline containing 5% (v/v) PEG400. DOX or DOX-hyd-LNA was intravenously administered to healthy BALB/c mice at doses of 9.2, 18.4, 27.6, 36.8, 46, and 55.2 μmol/kg (n = 4). The survival status and body weight of the mice were observed daily for 2 weeks. The MTD was defined as the dose resulting in no more than 15% body weight loss and no death of the mice for the 2 weeks after the drug was administered.[40−43]

2.2.11.2. In Vivo Antitumor Activity. HepG2 cells were subcutaneously implanted in the rear right flank of nude mice (1×10^7 cells/0.1 mL/animal). There were six nude mice in each group. Treatment was started on the 10th day when the tumor volume was about 80 mm^3. DOX or DOX-hyd-LNA was dissolved in normal saline containing 5% (v/v) PEG400. Free DOX (9.2 μmol/kg) or DOX-hyd-LNA (4.6 and 9.2 μmol/kg) was intravenously injected into tumor-bearing mice by the tail vein every 7 days for three doses (days 1, 7, and 14). The body weight of the mice was monitored every 3 days as a sign of systemic toxicity. The long (L) and short (W) diameter of the tumor were measured every 3 days with a caliper. The tumor volume was calculated as $LW^2/2$. On day 42, all surviving mice were euthanized.

dx.doi.org/10.1021/mp4004139 | Mol. Pharmaceutics 2014, 11, 1378−1390

2.2.11.3. Biodistribution. For the biodistribution study in vivo, tumor-bearing nude mice were treated with free DOX or DOX-hyd-LNA at a dose of 9.2 μmol/kg. Mice were euthanized at predetermined time intervals to collect their organs and tumor tissue. The tissues were rinsed with PBS and homogenized with water. The homogenate was centrifuged at 8000*g* for 15 min, and the supernatant was analyzed by HPLC–MS/MS.

2.2.12. Statistical Analysis. SigmaPlot 8.0 software was used to analyze the data. Student's *t* test was used to evaluate statistic significance, and $p < 0.05$ was considered to indicate a significant difference.

3. RESULTS AND DISCUSSION

3.1. Identification of DOX Conjugates. The typical HPLC chromatograms of DOX-hyd-LNA, DOX-ami-LNA, DOX-hyd-PA, and DOX-ami-PA are shown in Supporting Information Figure 7. The purity of DOX-hyd-LNA, DOX-ami-LNA, DOX-hyd-PA, and DOX-ami-PA was 98.7, 97.8, 98.2, and 97.3%, respectively. When LNA-$NHNH_2$ reacted with DOX to produce DOX-hyd-LNA, it was very important to control the amount of trifluoroacetic acid in the reaction mixture because excess trifluoroacetic acid could break the hydrazone bond between DOX and LNA. To avoid breaking DOX-hyd-LNA in the silica gel, triethylamine was added in the eluant.

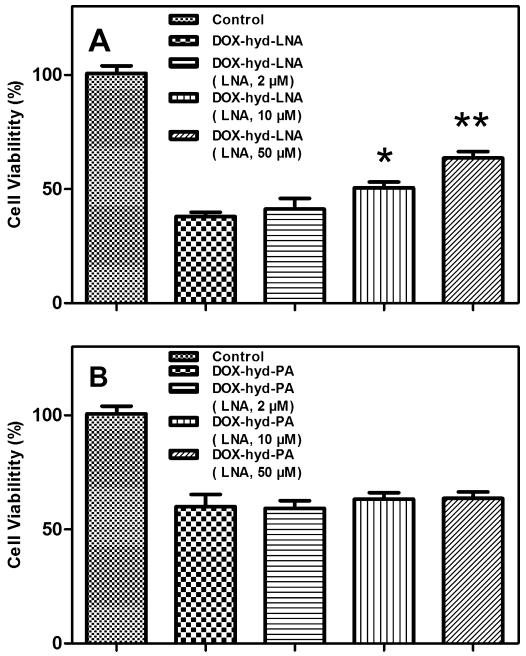

Figure 6. Effect of exogenous LNA on the viability of HepG2 cells. HepG2 cells were incubated with 8 μmol/L DOX-hyd-LNA (A) or the same dose of DOX-hyd-PA (B) for 48 h. *$p < 0.05$ vs DOX-hyd-LNA. $n = 5$.

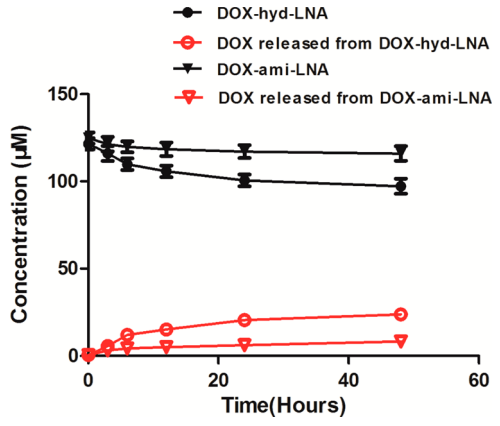

Figure 7. Stability of DOX-hyd-LNA and DOX-ami-LNA in rat serum. $n = 3$.

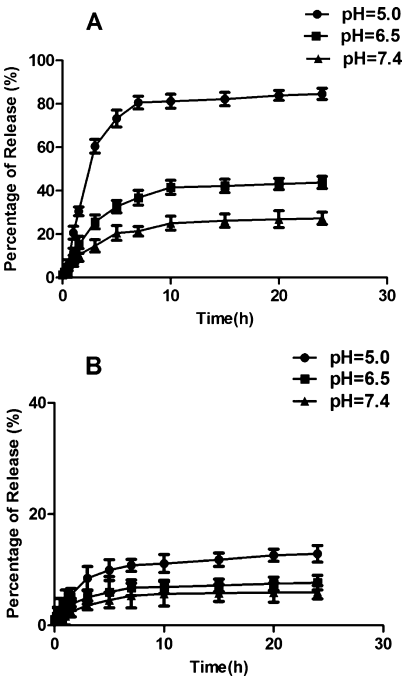

Figure 8. DOX-release characteristics from DOX-hyd-LNA (A) and DOX-ami-LNA (B) in medium with different pH values. $n = 3$.

A molecular description of DOX·HCl, DOX, and its fatty acid conjugates are presented in Table 2. There were three parameters that violated rule of five in the DOX conjugates.[44] As the length of the fatty acid substituent increase, the water solubility of the DOX derivative decreased. This was actually an expected result caused by the increased lipophilicity of the fatty acid substituent. The partition coefficient (Log P, octanol/water) was directly correlated to molecular weight, inversely correlated to the number of -OH and -NH groups (hydrogen-bond donors), and inversely correlated to water solubility.[45]

3.2. Cytotoxicity of DOX-hyd-LNA, DOX-ami-LNA, DOX-hyd-PA, and DOX-ami-PA. The cytotoxicity of free DOX, DOX-hyd-LNA, DOX-ami-LNA, DOX-hyd-PA, and DOX-ami-PA toward MCF-7, MDA-MB-231, and HepG2 cells was studied by MTT assay. As shown in Figure 5 and Table 3, DOX-hyd-LNA showed a higher cytotoxicity toward tumor cells than DOX, DOX-ami-LNA, DOX-hyd-PA, and DOX-ami-PA. The cytotoxicity of DOX toward tumor cell was higher than DOX-ami-LNA, DOX-hyd-PA, and DOX-ami-PA. This indicated that modification of the 3′ amino group in DOX with an unsaturated or saturated fatty acid led to a decrease in its antitumor activity. It also indicated that the connection of the saturated fatty acid (PA) with C13 of DOX by a hydrazone bond did not enhance the cytotoxicity of DOX. Furthermore, among the three tumor cell lines, DOX-hyd-LNA showed the highest cytotoxicity against HepG2 cells but the lowest

dx.doi.org/10.1021/mp4004139 | *Mol. Pharmaceutics* 2014, 11, 1378–1390

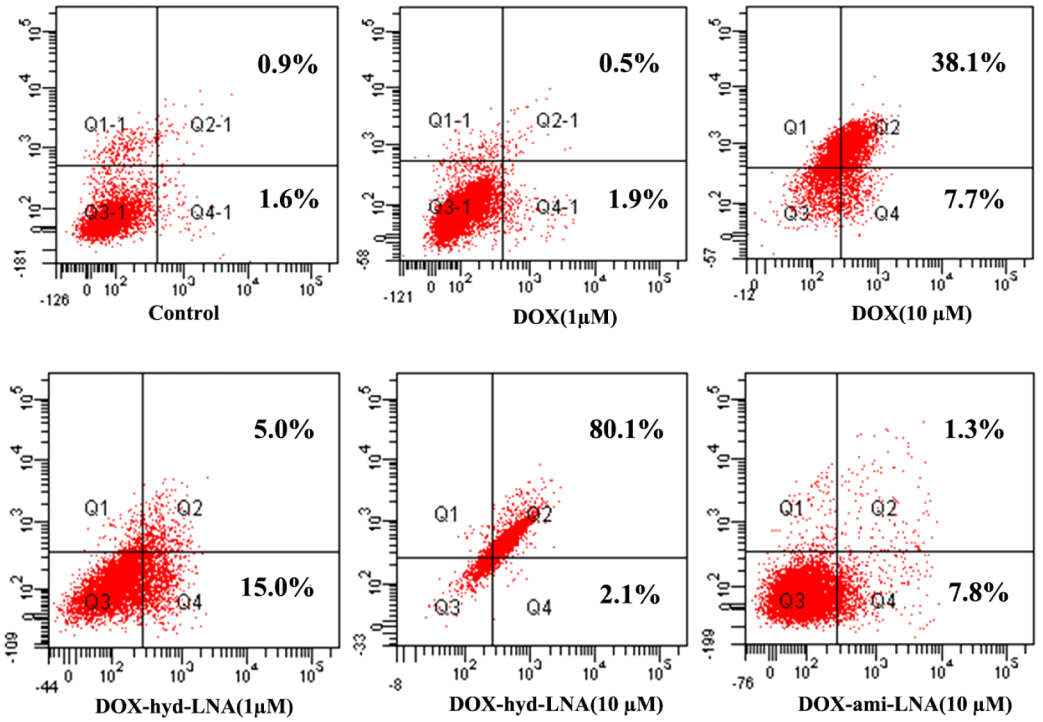

Figure 9. Apoptosis of HepG2 cells induced by DOX, DOX-hyd-LNA, and DOX-ami-LNA. DOX, DOX-ami-LNA, or DOX-hyd-LNA was incubated with HepG2 cells at 37 °C for 24 h.

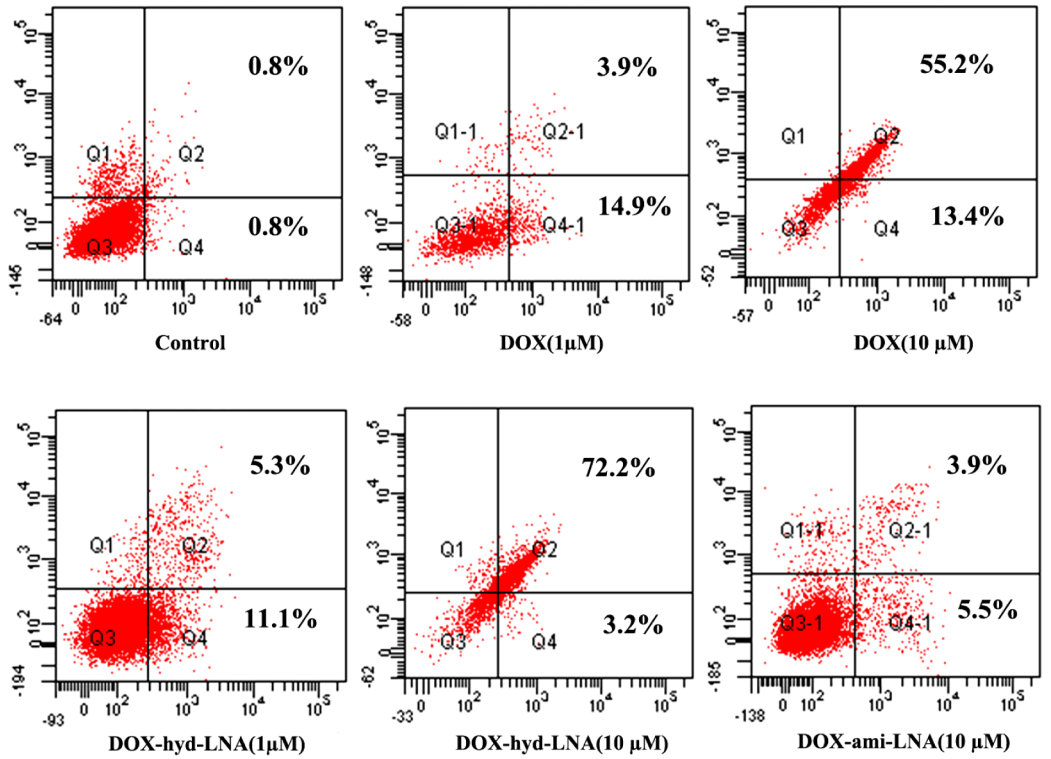

Figure 10. Apoptosis of MCF-7 cells induced by DOX, DOX-hyd-LNA, and DOX-ami-LNA. DOX, DOX-ami-LNA or DOX-hyd-LNA was incubated with MCF-7 cells at 37 °C for 24 h.

cytotoxicity toward MDA-MB-231 cells. It was anticipated that the DOX-hyd-LNA and DOX-ami-LNA would be taken up by the tumor cells through LNA-mediated endocytosis and localized in an acidic organelle, such as an endosome or lysosome, from which DOX would be released from DOX-hyd-LNA and DOX-ami-LNA and subsequently diffuse into the nucleus.[46,47] The effect of exogenous LNA on the cytotoxicity of DOX-hyd-LNA is shown in Figure 6. When HepG2 cells were incubated with DOX-hyd-LNA and different concentration of exogenous free LNA for 48 h, the cytotoxicity of

dx.doi.org/10.1021/mp4004139 | *Mol. Pharmaceutics* 2014, 11, 1378−1390

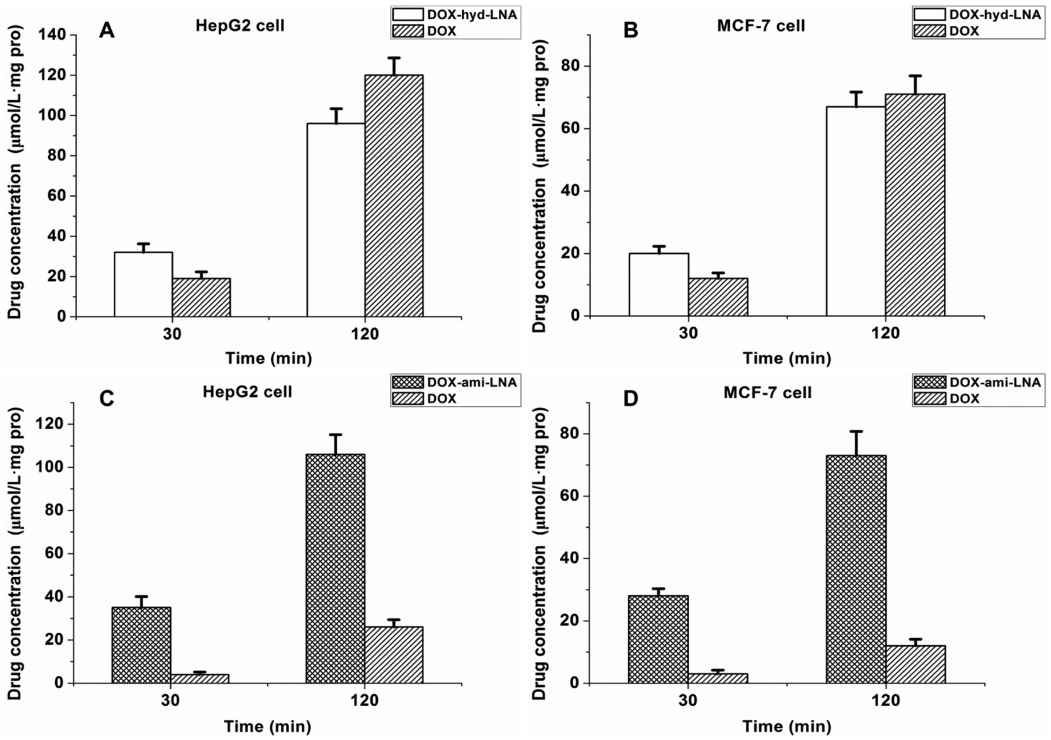

Figure 11. Quantitative uptake and DOX-release characteristic of DOX-hyd-LNA and DOX-ami-LNA in HepG2 and MCF-7 cells at 37 °C: (A) 20 μmol/L DOX-hyd-LNA incubated with HepG2 cells, (B) 20 μmol/L DOX-hyd-LNA incubated with MCF-7 cells, (C) 20 μmol/L DOX-ami-LNA incubated with HepG2 cells, and (D) 20 μmol/L DOX-ami-LNA incubated with MCF-7 cells. n = 5.

DOX-hyd-LNA on HepG2 cells decreased in a dose-dependent manner. Meanwhile, the cytotoxicity of DOX-hyd-PA on HepG2 cells was not affected by exogenous LNA. This implied that LNA plays an important role in the cytotoxicity of DOX-hyd-LNA toward HepG2 cells.

The cytotoxicity of DOX-hyd-LNA, DOX-ami-LNA, DOX-hyd-PA, DOX-ami-PA, and free DOX on HUVECs is shown in Table 3 and Figure 5. The cytotoxicity of DOX-hyd-LNA toward HUVECs was significantly lower than that of free DOX. This indicated that DOX-hyd-LNA exhibited selectivity for tumor cells. Kratz et al. cultured an acid-sensitive transferrin−DOX conjugate with HUVECs, and the result indicated that the cytotoxicity of transferrin−DOX conjugate toward HUVECs was significantly less than that of the free DOX.[48] Additionally, Shahin et al. found that p160-decorated micelles (encapsulated paclitaxel) showed greater cytotoxicity toward MDA-MB-435 cells than toward HUVECs or MCF10A cells.[49]

In addition to a small molecule PUFA−DOX conjugate, Rodrigues et al. synthesized a series of DOX-poly(ethylene glycol) (PEG) conjugates by an amide or a hydrazone bond in which the DOX maleimide derivatives were linked with α-methoxy-PEG-thiopropionic acid amide (MW 20 000 Da), α,ω-bis-thiopropionic acid amide PEG (MW 20 000 Da), or α-tert-butoxy-PEG-thiopropionic acid amide (MW 70 000 Da).[50] The hydrazone bond conjugates showed antitumor activity toward human BXF T24 bladder carcinoma and LXFL 529L lung cancer cells, but the amide bond conjugates exhibited no antitumor activity in vitro.[50] In our group, DOX was connected with HOOC-PEG-COOH by a hydrazone bond (PEG-hyd-DOX) or an amide bond (PEG-ami-DOX) to improve the therapeutic index of DOX. The results showed that the acid-sensitive PEG-hyd-DOX conjugate released free DOX in the acidic environment of the tumor.[51] These results implied that the hydrazone bond is crucial for DOX conjugates to exert their efficacy.

3.3. Hydrolysis of DOX-hyd-LNA and DOX-ami-LNA in Rat Serum. The hydrolytic characteristics of DOX-hyd-LNA and DOX-ami-LNA in rat serum are shown in Figure 7. The results indicated that the concentration of DOX-hyd-LNA decreased 23% in 24 h and that a small amount of DOX was released during the period from 24 to 48 h. Compared with DOX-hyd-LNA, DOX-ami-LNA was more stable in rat serum after 48 h.

3.4. DOX Release from DOX-hyd-LNA and DOX-ami-LNA in Medium with Different pH Values in Vitro. The drug-release characteristics of DOX-hyd-LNA and DOX-ami-LNA in medium with different pH values at 37 °C were investigated. The results are shown in Figure 8. The time-dependent chromatograms of the hydrolysis studies are shown in Supporting Information Figures 8 and 9. On the one hand, the rate at which DOX was released from DOX-hyd-LNA was closely related to the pH of the medium. DOX-hyd-LNA released 81% of the conjugated DOX in pH 5.0 medium in 4 h, but it released 22% of the conjugated DOX in pH 7.4 medium in 24 h. The relatively slow DOX release rate of DOX-hyd-LNA in pH 7.4 medium should ensure the relative stability of DOX-hyd-LNA in the bloodstream. The faster DOX release rate of DOX-hyd-LNA in acidic medium mimicked the burst release of DOX from DOX-hyd-LNA in the endosomal/lysosomal compartments of the tumor cells.

On the other hand, the rate at which DOX was released from DOX-ami-LNA was independent of the pH of the medium. DOX-ami-LNA released 5% of conjugated DOX in pH 7.4 medium in 10 h, and 11% of conjugated DOX was released in pH 5.0 medium in 10 h. These results implied that it is difficult for DOX-ami-LNA to release DOX in tumor cells. Con-

dx.doi.org/10.1021/mp4004139 | Mol. Pharmaceutics 2014, 11, 1378−1390

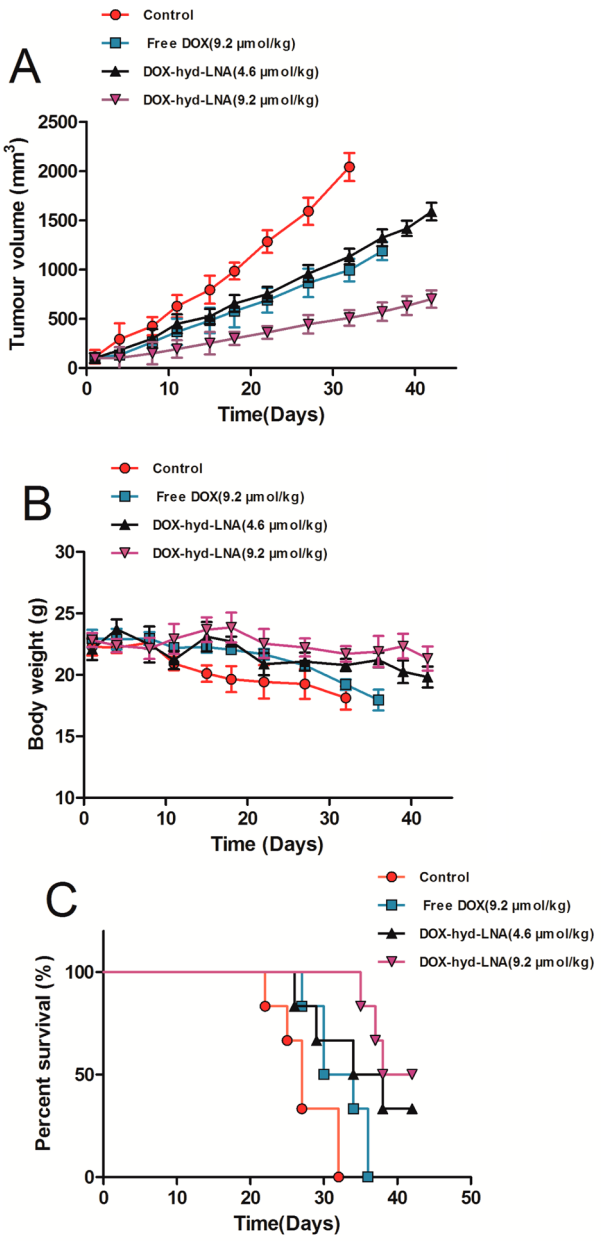

Figure 12. Antitumor activity of DOX-hyd-LNA in vivo. Athymic nude mice xenografted with HepG2 cells were intravenously injected with different doses of DOX-hyd-LNA (4.6 and 9.2 μmol/kg) and one dose of DOX (9.2 μmol/kg). Treatment was initiated when the tumor volume was about 80 mm^3. n = 6. Tumor-bearing mice were treated with normal saline (control), DOX, or DOX-hyd-LNA by tail vein injection every 7 days (days 1, 7, and 14). (A) Tumor volume changes in tumor-bearing nude mice, (B) body weight changes in tumor-bearing nude mice, (C) survival curve of tumor-bearing nude mice.

sequently, DOX-hyd-LNA showed higher cytotoxicity toward tumor cells than DOX-ami-LNA.

3.5. Cell Apoptosis Induced by DOX-hyd-LNA and DOX-ami-LNA. DOX-hyd-LNA and DOX-ami-LNA were incubated with HepG2 and MCF-7 cells for 24 h, and the apoptotic cells were detected by flow cytometry. As shown in Figures 9 and 10, DOX-hyd-LNA induced apoptosis in HepG2 and MCF-7 cells in a dose-dependent manner. Compared with free DOX and DOX-ami-LNA, DOX-hyd-LNA induced significantly more apoptosis. Additionally, compared with MCF-7 cells, DOX-hyd-LNA induced more apoptosis in HepG2 cells. These data are consistent with the results of cytotoxicity experiment as well as with the drug-release characteristics of DOX-hyd-LNA and DOX-ami-LNA in vitro.

Table 4. Statistic Analysis of the Survival of Tumor-Bearing Mice

treatment group	median survival (days)	mean survival (days)	maximal survival (days)	p
control	27	26.60 ± 1.63	32	
free DOX (9.2 μmol/kg)	30	31.40 ± 1.60	36	0.069[a]
DOX-hyd-LNA (4.6 μmol/kg)	34	33.80 ± 2.59	42	0.375[b]
DOX-hyd-LNA (9.2 μmol/kg)	38	38.80 ± 1.25	42	0.007[b]

[a]Compared with control. [b]Compared with free DOX.

3.6. Uptake of DOX-hyd-LNA and DOX-ami-LNA in MCF-7 and HepG2 Cells. After MCF-7 and HepG2 cells were incubated with DOX-hyd-LNA or DOX-ami-LNA (20 μmol/L) for 30 and 120 min, the intracellular amount of DOX, DOX-hyd-LNA, or DOX-ami-LNA was detected by HPLC−MS/MS. As shown in Figure 11, both DOX-hyd-LNA and DOX-ami-LNA were taken up by MCF-7 and HepG2 cells in a time-dependent manner. Meanwhile, a large amount of DOX was released from DOX-hyd-LNA in HepG2 and MCF-7 cells, but a small amount of DOX was released from DOX-ami-LNA in MCF-7 and HepG2 cells. Compared with MCF-7 cells, a large amount of DOX-hyd-LNA and DOX-ami-LNA was accumulated in HepG2 cells, and a greater amount of DOX was released from DOX-hyd-LNA in HepG2 cells. These results provide an explanation as to why DOX-hyd-LNA exhibited higher cytotoxicity toward HepG2 cells than MCF-7 cells.

It has been established that PUFAs are taken up much more readily by tumor cells than by normal cells.[22,52] In addition, PUFAs are able to be inserted quickly into the membrane of tumor cells, damaging the structure and fluidity of the cell membrane.[53] This implies that PUFAs are able to enhance the uptake of antitumor drugs by tumor cells,increasing the sensitivity of chemotherapy drugs.[54] A daunomycin−arachidonic acid conjugate showed greater cytotoxicity toward hepatoma cells than free daunomycin. However, the daunomycin−arachidic acid (a saturated fatty acid) conjugate exhibited the same antitumor activity as free daunomycin.[55] This indicated that arachidonic acid exerts an important role for the antitumor activity of the daunomycin−arachidonic acid conjugate. Moreover, when 4′-demethyldeoxypodophyllotoxin (DDPT) was conjugated with an unsaturated fatty acid by an ester bond, its antitumor activity in vivo was increased without any effect on body weight loss.[56]

3.7. MTD of DOX-hyd-LNA. There was no remarkable reduction in body weight or any other toxic reaction in mice treated with DOX-hyd-LNA at doses of 9.2−36.8 μmol/kg in the 2 weeks following its injection. The 46 μmol/kg DOX-hyd-LNA treatment resulted in body weight reduction (<11%) during the first week, but the body weight returned to normal as soon as the experiment ended. The 18.4 μmol/kg free DOX treatment caused body weight reduction (<14%) without any death of the mice. The 27.6 μmol/kg free DOX treatment resulted in a quick reduction in the body weight, and all animals died in this group within 2 weeks. Therefore, the MTD of DOX-hyd-LNA and free DOX in BLAB/c mice was, for a single

dx.doi.org/10.1021/mp4004139 | Mol. Pharmaceutics 2014, 11, 1378−1390

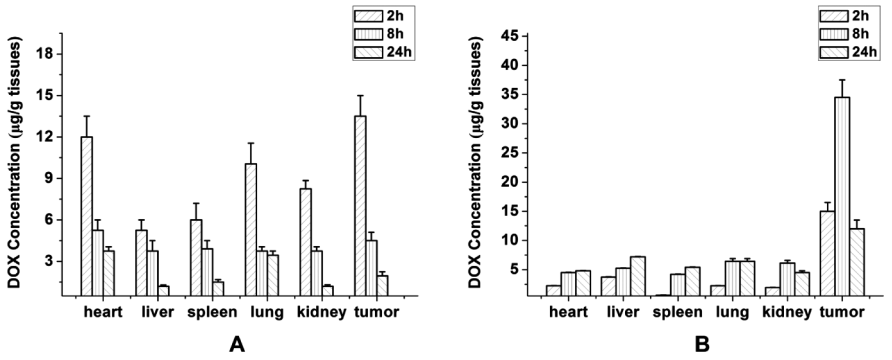

Figure 13. Distribution of DOX in tumor-bearing nude mice after intravenous injection of free DOX (A) or DOX-hyd-LNA (B). n = 5.

injection, approximately 46 and 18.4 μmol/kg, respectively. The MTD value of DOX presented in this article is consistent with previous literature reports.[43,57−60] Doxil is a very stable liposome of DOX used in the clinic. It has been reported that the MTD of doxil is almost the same as free DOX in dogs but is lower than free DOX in mice.[61,62]

3.8. In Vivo Antitumor Activity. Tumor-bearing nude mice were used to investigate the antitumor activity of DOX-hyd-LNA in vivo. An equimolar amount of DOX and DOX-hyd-LNA was administered through the tail vein. The antitumor activity of DOX-hyd-LNA is shown in Figure 12 and Table 4. A time-related tumor volume increase was observed in all groups. Although neither DOX nor DOX-hyd-LNA could completely stop the growth of the tumor, the tumors in the drug-treated groups showed an obvious growth retardation in a dose-dependent manner. This result is consistent with previous observations in the literature.[40,63,64] Compared with DOX, DOX-hyd-LNA exhibited a stronger tumor growth inhibition. The cellular uptake experiment indicated that a large amount of DOX was released from DOX-hyd-LNA in HepG2 cells, which exerted an important role in delaying the growth of the tumor in vivo.

When tumor-bearing nude mice were treated with free DOX (9.2 μmol/kg), the activity and body weight of the mice were remarkably reduced. However, no indication of a significant toxic reaction was discovered in tumor-bearing mice when treated with an equimolar amount of DOX-hyd-LNA. This implied that treatment with DOX-hyd-LNA enhances therapeutic efficacy with less systemic toxicity.

INNO-206 is another hydrazone bond-based derivative of DOX in which doxorubicin is connected with 6-maleimidocaproic acid at its C13 keto-position through a hydrazone bond. INNO-206 can specifically react with cysteine-34 of human serum albumin to form an albumin-binding DOX prodrug. The albumin-binding DOX is able to accumulate in tumor tissue by the enhanced permeability and retention (EPR) effect, and the DOX can be released in an acidic environment such as tumor tissue or tumor cell endosomal or lysosomal compartments.[65] INNO-206 has entered phase II clinic trials for the treatment of sarcoma.[66]

3.9. Drug Biodistribution. After free DOX or DOX-hyd-LNA was intravenously administered, the biodistribution of DOX in tumor-bearing nude mice was assessed and is shown in Figure 13. DOX typically accumulated in the liver, heart, spleen, lung, kidney, and tumor tissue after free DOX or DOX-hyd-LNA was administered. Compared with free DOX, treatment with an equimolar amount of DOX-hyd-LNA greatly increased the content of DOX in the tumor tissue and significantly decreased the content of DOX in heart. The level of DOX in the tumor tissue was 12 μg/g tissue, and this level was sustained for 24 h. The longer exposure to a high DOX concentration led to the improvement of the antitumor activity of DOX-hyd-LNA.

In the human body, fatty acids are transported through the vascular and lymphatic systems. Fatty acids need to bind plasma proteins to increase their concentration in vascular and interstitial compartments because of their poor solubility in water. Human plasma albumin is the main fatty acid-binding protein in blood. Plasma albumin possesses high-affinity binding sites for fatty acids to enhance the concentration of fatty acids in blood.[67] Thus, fatty acids can be used to prolong the half-life of an antitumor drug and peptide in vivo.[68−70]

DHA−paclitaxel (taxoprexin) was shown to be stable in plasma and was extensively bonded with human plasma albumin in vitro. The plasma protein binding rate of DHA−paclitaxel was 99.600 ± 0.057% in human plasma, which resulted in a small distribution volume and slow systemic clearance. The plasma protein binding property of DHA−paclitaxel is favorable for enhancing its antitumor efficacy.[70] Pharmacokinetic studies showed that DHA−paclitaxel significantly increased the content of paclitaxel in tumor tissue compared with paclitaxel at an equimolar dose, which was due to the EPR effect of plasma protein-bound DHA−paclitaxel. Additionally, DHA−paclitaxel was relatively stable in blood circulation, and only 0.5% of paclitaxel was released from DHA−paclitaxel in blood. Thus, the increased accumulation of paclitaxel in tumor tissue and the relative stability of DHA−paclitaxel in blood resulted in an enhancement of the therapeutic efficacy of DHA−paclitaxel in tumor-bearing mouse model.[71] The safety of DHA−paclitaxel has been demonstrated in metastatic uveal melanoma patients.[72,73]

The plasma protein binding rate of DOX-hyd-LNA was 98.7 ± 1.1% in rat plasma. Determining whether the increased distribution of DOX in tumor tissue was caused by the high plasma protein binding rate of DOX-hyd-LNA still needs further investigation.

4. CONCLUSIONS

Compared with DOX, DOX-hyd-LNA exhibited improved antitumor activity with less toxicity in vitro and in vivo. These results were due to the stability of DOX-hyd-LNA in serum, the increased distribution of DOX in tumor tissues, and the large amount of DOX released in tumor cells. Thus, DOX-hyd-LNA is a compound with great potential, and we expect that it will be researched further as a cancer-targeting therapy.

■ ASSOCIATED CONTENT

Supporting Information

MS and ^{1}H NMR data for NBoc-LNA hydrazine, LNA-$NHNH_2$, DOX-hyd-LNA, PA-$NHNH_2$, DOX-hyd-PA, and DOX-ami-PA; HPLC chromatograms of DOX, DOX-hyd-LNA, DOX-ami-LNA, DOX-hyd-PA, and DOX-ami-PA; and time-dependent chromatograms of hydrolysis of DOX-hyd-LNA and DOX-ami-LNA in pH 5.0 medium. This material is available free of charge via the Internet at http://pubs.acs.org.

■ AUTHOR INFORMATION

Corresponding Author

*(S.-y.Z.) Tel.: +86 (0)2984776783; Fax: +86 (0)2984779212; E-mail: zhousy@fmmu.edu.cn.

Author Contributions

‖C.-h.L. and W.-l.Y. contributed equally to this work.

Notes

The authors declare no competing financial interest.

■ ACKNOWLEDGMENTS

This research was sponsored by the Science and Technology Innovation Project of Shaanxi (2012KTCL03-18) and the Shaanxi Natural Science Foundation (2013JQ4026).

■ REFERENCES

(1) Lenaz, L.; Page, J. A. Cardiotoxicity of adriamycin and related anthracyclines. *Cancer Treat. Rev.* **1976**, *3*, 111−120.

(2) Weiss, R. B. The anthracyclines: Will we ever find a better doxorubicin? *Semin. Oncol.* **1992**, *19*, 670−686.

(3) Johnson, B. A.; Cheang, M. S.; Goldenberg, G. J. Comparison of adriamycin uptake in chick embryo heart and liver cells an murine L5178Y lymphoblasts in vitro: Role of drug uptake in cardiotoxicity. *Cancer Res.* **1986**, *46*, 218−223.

(4) Lampidis, T. J.; Johnson, L. V.; Israel, M. Effects of adriamycin on rat heart cells in culture: Increased accumulation and nucleoli fragmentation in cardiac muscle v. non-muscle cells. *J. Mol. Cell. Cardiol.* **1981**, *13*, 913−924.

(5) Khandare, J. J.; Minko, T. Antibodies and peptides in cancer therapy. *Crit. Rev. Ther. Drug Carrier Syst.* **2006**, *23*, 401−435.

(6) Jayant, S.; Khandare, J. J.; Wang, Y.; Singh, A. P.; Vorsa, N.; Minko, T. Targeted sialic acid-doxorubicin prodrugs for intracellular delivery and cancer treatment. *Pharm. Res.* **2007**, *24*, 2120−2130.

(7) Kumar, S. A.; Peter, Y. A.; Nadeau, J. L. Facile biosynthesis, separation and conjugation of gold nanoparticles to doxorubicin. *Nanotechnology* **2008**, *19*, 495101.

(8) You, J.; Zhang, G.; Li, C. Exceptionally high payload of doxorubicin in hollow gold nanospheres for near-infrared light-triggered drug release. *ACS Nano* **2010**, *4*, 1033−1041.

(9) Barenholz, Y. Doxil(®)−the first FDA-approved nano-drug: Lessons learned. *J. Controlled Release* **2012**, *160*, 117−134.

(10) Zhu, S.; Hong, M.; Zhang, L.; Tang, G.; Jiang, Y.; Pei, Y. PEGylated PAMAM dendrimer-doxorubicin conjugates: In vitro evaluation and in vivo tumor accumulation. *Pharm. Res.* **2010**, *27*, 161−174.

(11) Ibsen, S.; Zahavy, E.; Wrasdilo, W.; Berns, M.; Chan, M.; Esener, S. A novel doxorubicin prodrug with controllable photolysis activation for cancer chemotherapy. *Pharm. Res.* **2010**, *27*, 1848−1860.

(12) Chhikara, B. S.; Parang, K. Development of cytarabine prodrugs and delivery systems for leukemia treatment. *Expert Opin. Drug Delivery* **2010**, *7*, 1399−1414.

(13) Jaracz, S.; Chen, J.; Kuznetsova, L. V.; Ojima, I. Recent advances in tumor-targeting anticancer drug conjugates. *Bioorg. Med. Chem.* **2005**, *13*, 5043−5054.

(14) Swaan, P. W. Recent advances in intestinal macromolecular drug delivery via receptor-mediated transport pathways. *Pharm. Res.* **1998**, *15*, 826−834.

(15) Allen, T. M. Ligand-targeted therapeutics in anticancer therapy. *Nat. Rev. Cancer* **2002**, *2*, 750−763.

(16) Wu, G. S.; Lu, J. J.; Guo, J. J.; Huang, M. Q.; Gan, L.; Chen, X. P.; Wang, Y. T. Synergistic anti-cancer activity of the combination of dihydroartemisinin and doxorubicin in breast cancer cells. *Pharmacol. Rep.* **2013**, *65*, 453−459.

(17) Wigmore, S. J.; Ross, J. A.; Falconer, J. S.; Plester, C. E.; Tisdale, M. J.; Carter, D. C.; Fearon, K. C. The effect of polyunsaturated fatty acids on the progress of cachexia in patients with pancreatic cancer. *Nutrition* **1996**, *12*, S27−S30.

(18) Hawkins, R. A.; Sangster, K.; Arends, M. J. Apoptotic death of pancreatic cancer cells induced by polyunsaturated fatty acids varies with double bond number and involves an oxidative mechanism. *J. Pathol.* **1998**, *185*, 61−70.

(19) Siddiqui, R. A.; Harvey, K. A.; Xu, Z.; Bammerlin, E. M.; Walker, C.; Altenburg, J. D. Docosahexaenoic acid: A natural powerful adjuvant that improves efficacy for anticancer treatment with no adverse effects. *BioFactors* **2011**, *37*, 399−412.

(20) Kuan, C. Y.; Walker, T. H.; Luo, P. G.; Chen, C. F. Long-chain polyunsaturated fatty acids promote paclitaxel cytotoxicity via inhibition of the MDR1 gene in the human colon cancer Caco-2 cell line. *J. Am. Coll. Nutr* **2011**, *30*, 265−273.

(21) Merendino, N.; Costantini, L.; Manzi, L.; Molinari, R.; D'Eliseo, D.; Velotti, F. Dietary omega-3 polyunsaturated fatty acid DHA: A potential adjuvant in the treatment of cancer. *BioMed Res. Int.* **2013**, *2013*, 310186-1−310186-11.

(22) Sauer, L. A.; Dauchy, R. T.; Blask, D. E. Mechanism for the antitumor and anticachectic effects of n-3 fatty acids. *Cancer Res.* **2000**, *60*, 5289−5295.

(23) Koralek, D. O.; Peters, U.; Andriole, G.; Reding, D.; Kirsh, V.; Subar, A.; Schatzkin, A.; Hayes, R.; Leitzmann, M. F. A prospective study of dietary alpha-linolenic acid and the risk of prostate cancer (United States). *Cancer, Causes Control* **2006**, *17*, 783−791.

(24) Coakley, M.; Banni, S.; Johnson, M. C.; Mills, S.; Devery, R.; Fitzgerald, G.; Paul Ross, R.; Stanton, C. Inhibitory effect of conjugated alpha-linolenic acid from bifidobacteria of intestinal origin on SW480 cancer cells. *Lipids* **2009**, *44*, 249−256.

(25) Kuznetsova, L.; Chen, J.; Sun, L.; Wu, X.; Pepe, A.; Veith, J. M.; Pera, P.; Bernacki, R. J.; Ojima, I. Syntheses and evaluation of novel fatty acid-second-generation taxoid conjugates as promising anticancer agents. *Bioorg. Med. Chem. Lett.* **2006**, *16*, 974−977.

(26) Tanmahasamut, P.; Liu, J.; Hendry, L. B.; Sidell, N. Conjugated linoleic acid blocks estrogen signaling in human breast cancer cells. *J. Nutr.* **2004**, *134*, 674−680.

(27) Bedikian, A. Y.; DeConti, R. C.; Conry, R.; Agarwala, S.; Papadopoulos, N.; Kim, K. B.; Ernstoff, M. Phase 3 study of docosahexaenoic acid-paclitaxel versus dacarbazine in patients with metastatic malignant melanoma. *Ann. Oncol.* **2011**, *22*, 787−793.

(28) Wang, Y.; Li, L.; Jiang, W.; Yang, Z.; Zhang, Z. Synthesis and preliminary antitumor activity evaluation of a DHA and doxorubicin conjugate. *Bioorg. Med. Chem. Lett.* **2006**, *16*, 2974−2977.

(29) Chhikara, B. S.; Mandal, D.; Parang, K. Synthesis, anticancer activities, and cellular uptake studies of lipophilic derivatives of doxorubicin succinate. *J. Med. Chem.* **2012**, *55*, 1500−1510.

(30) Effenberger, K.; Breyer, S.; Schobert, R. Modulation of doxorubicin activity in cancer cells by conjugation with fatty acyl and terpenyl hydrazones. *Eur. J. Med. Chem.* **2010**, *45*, 1947−1954.

(31) Huan, M. L.; Zhou, S. Y.; Teng, Z. H.; Zhang, B. L.; Liu, X. Y.; Wang, J. P.; Mei, Q. B. Conjugation with alpha-linolenic acid improves cancer cell uptake and cytotoxicity of doxorubicin. *Bioorg. Med. Chem. Lett.* **2009**, *19*, 2579−2584.

(32) Zhai, L.; Zhang, P.; Sun, R. Y.; Liu, X. Y.; Liu, W. G.; Guo, X. L. Cytoprotective effects of CSTMP, a novel stilbene derivative, against H_2O_2-induced oxidative stress in human endothelial cells. *Pharmacol. Rep.* **2011**, *63*, 1469−1480.

(33) Maeda, R.; Noiri, E.; Isobe, H.; Homma, T.; Tanaka, T.; Negishi, K.; Doi, K.; Fujita, T.; Nakamura, E. A water-soluble fullerene vesicle alleviates angiotensin II-induced oxidative stress in human umbilical venous endothelial cells. *Hypertens. Res.* **2008**, *31*, 141−151.

(34) Park, H. J.; Zhang, Y.; Georgescu, S. P.; Johnson, K. L.; Kong, D.; Galper, J. B. Human umbilical vein endothelial cells and human dermal microvascular endothelial cells offer new insights into the relationship between lipid metabolism and angiogenesis. *Stem Cell Rev.* **2006**, *2*, 93−102.
(35) Alkhalaf, M. Resveratrol-induced growth inhibition in MDA-MB-231 breast cancer cells is associated with mitogen-activated protein kinase signaling and protein translation. *Eur. J. Cancer Prev.* **2007**, *16*, 334−341.
(36) Martowicz, A.; Spizzo, G.; Gastl, G.; Untergasser, G. Phenotype-dependent effects of EpCAM expression on growth and invasion of human breast cancer cell lines. *BMC Cancer* **2012**, *12*, 501-1−501-15.
(37) Pozo-Guisado, E.; Merino, J. M.; Mulero-Navarro, S.; Lorenzo-Benayas, M. J.; Centeno, F.; Alvarez-Barrientos, A.; Salguero, P. M. F. Resveratrol-induced apoptosis in MCF-7 human breast cancer cells involves a caspase-independent mechanism with downregulation of Bcl-2 and NF-κB. *Int. J. Cancer* **2005**, *115*, 74−84.
(38) Lancon, A.; Delma, D.; Osman, H.; Thenot, J.-P.; Latruffe, B. J. Human hepatic cell uptake of resveratrol: Involvement of both passive diffusion and carrier-mediated process. *Biochem. Biophys. Res. Commun.* **2004**, *316*, 1132−1137.
(39) Lancon, A.; Hanet, N.; Jannin, B.; Delmas, D.; Heydel, J. M.; Lizard, G.; Chagnon, M. C.; Artur, Y.; Latruffe, N. Resveratrol in human hepatoma HepG2 cells: Metabolism and inducibility of detoxifying enzymes. *Drug Metab. Dispos.* **2007**, *35*, 699−703.
(40) Xiao, K.; Luo, J.; Li, Y.; Lee, J. S.; Fung, G.; Lam, K. S. PEG-oligocholic acid telodendrimer micelles for the targeted delivery of doxorubicin to B-cell lymphoma. *J. Controlled Release* **2011**, *155*, 272−281.
(41) Lo, S. T.; Stern, S.; Clogston, J. D.; Zheng, J.; Adiseshaiah, P. P.; Dobrovolskaia, M.; Lim, J.; Patri, A. K.; Sun, X.; Simanek, E. E. Biological assessment of triazine dendrimer: Toxicological profiles, solution behavior, biodistribution, drug release and efficacy in a PEGylated, paclitaxel construct. *Mol. Pharmaceutics* **2010**, *7*, 993−1006.
(42) Vanhoefer, U.; Cao, S.; Harstrick, A.; Seeber, S.; Rustum, Y. Comparative antitumor efficacy of docetaxel and paclitaxel in nude mice bearing human tumor xenografts that overexpress the multidrug resistance protein (MRP). *Ann. Oncol.* **1997**, *8*, 1221−1228.
(43) Lee, C. C.; Gillies, E. R.; Fox, M. E.; Guillaudeu, S. J.; Frechet, J. M.; Dy, E. E.; Szoka, F. C. A single dose of doxorubicin-functionalized bow-tie dendrimer cures mice bearing C-26 colon carcinomas. *Proc. Natl. Acad. Sci. U.S.A.* **2006**, *103*, 16649−16654.
(44) Lipinski, C. A.; Lombardo, F.; Dominy, B. W.; Feeney, P. J. Experimental and computational approaches to estimate solubility and permeability in drug discovery and development settings. *Adv. Drug Delivery Rev.* **2001**, *46*, 3−26.
(45) Bartzatt, R. Use of pattern recognition analysis to identify underlying relationships of doxorubicin derivatives optimized for breast cancer treatment. *ISRN Oncol.* **2011**, 585192-1−585192-6.
(46) Gillies, E. R.; Frechet, J. M. pH-responsive copolymer assemblies for controlled release of doxorubicin. *Bioconjugate Chem.* **2005**, *16*, 361−368.
(47) Lee, C. C.; Cramer, A. T.; Szoka, F. C., Jr.; Frechet, J. M. An intramolecular cyclization reaction is responsible for the in vivo inefficacy and apparent pH insensitive hydrolysis kinetics of hydrazone carboxylate derivatives of doxorubicin. *Bioconjugate Chem.* **2006**, *17*, 1364−1368.
(48) Kratz, F.; Beyer, U.; Roth, T.; Tarasova, N.; Collery, P.; Lechenault, F.; Cazabat, A.; Schumacher, P.; Unger, C.; Falken, U. Transferrin conjugates of doxorubicin: synthesis, characterization, cellular uptake, and in vitro efficacy. *J. Pharm. Sci.* **1998**, *87*, 338−346.
(49) Shahin, M.; Ahmed, S.; Kaur, K.; Lavasanifar, A. Decoration of polymeric micelles with cancer-specific peptide ligands for active targeting of paclitaxel. *Biomaterials* **2011**, *32*, 5123−5133.
(50) Rodrigues, P. C.; Beyer, U.; Schumacher, P.; Roth, T.; Fiebig, H. H.; Unger, C.; Messori, L.; Orioli, P.; Paper, D. H.; Mulhaupt, R.; Kratz, F. Acid-sensitive polyethylene glycol conjugates of doxorubicin: Preparation, in vitro efficacy and intracellular distribution. *Bioorg. Med. Chem.* **1999**, *7*, 2517−2524.
(51) Huan, M.; Zhang, B.; Teng, Z.; Cui, H.; Wang, J.; Liu, X.; Xia, H.; Zhou, S.; Mei, Q. In vitro and in vivo antitumor activity of a novel pH-activated polymeric drug delivery system for doxorubicin. *PLoS One* **2012**, *7*, e44116-1−e44116-11.
(52) Sauer, L. A.; Dauchy, R. T. The effect of omega-6 and omega-3 fatty acids on 3H-thymidine incorporation in hepatoma 7288CTC perfused in situ. *Br. J. Cancer* **1992**, *66*, 297−303.
(53) Grammatikos, S. I.; Subbaiah, P. V.; Victor, T. A.; Miller, W. M. n-3 and n-6 fatty acid processing and growth effects in neoplastic and non-cancerous human mammary epithelial cell lines. *Br. J. Cancer* **1994**, *70*, 219−227.
(54) Diomede, L.; Colotta, F.; Piovani, B.; Re, F.; Modest, E. J.; Salmona, M. Induction of apoptosis in human leukemic cells by the ether lipid 1-octadecyl-2-methyl-rac-glycero-3-phosphocholine. A possible basis for its selective action. *Int. J. Cancer* **1993**, *53*, 124−130.
(55) Sasaki, T.; Tsukada, Y.; Deutsch, H. F.; Hirai, H. Daunomycin−arachidonic acid complex as a potential new antitumor agent. *Cancer Chemother. Pharmacol.* **1984**, *13*, 75−77.
(56) You, Y. J.; Kim, Y.; Nam, N. H.; Ahn, B. Z. Antitumor activity of unsaturated fatty acid esters of 4′-demethyldeoxypodophyllotoxin. *Bioorg. Med. Chem. Lett.* **2003**, *13*, 2629−2632.
(57) Gabizon, A.; Meshorer, A.; Barenholz, Y. Comparative long-term study of the toxicities of free and liposome-associated doxorubicin in mice after intravenous administration. *J. Natl. Cancer Inst.* **1986**, *77*, 459−469.
(58) Bae, Y.; Nishiyama, N.; Fukushima, S.; Koyama, H.; Yasuhiro, M.; Kataoka, K. Preparation and biological characterization of polymeric micelle drug carriers with intracellular pH-triggered drug release property: Tumor permeability, controlled subcellular drug distribution, and enhanced in vivo antitumor efficacy. *Bioconjugate Chem.* **2005**, *16*, 122−130.
(59) Boven, E.; Schluper, H. M.; Erkelens, C. A.; Pinedo, H. M. Doxorubicin compared with related compounds in a nude mouse model for human ovarian cancer. *Eur. J. Cancer* **1990**, *26*, 983−986.
(60) Breistol, K.; Hendriks, H. R.; Fodstad, O. Superior therapeutic efficacy of N-L-leucyl-doxorubicin versus doxorubicin in human melanoma xenografts correlates with higher tumour concentrations of free drug. *Eur. J. Cancer* **1999**, *35*, 1143−1149.
(61) Vail, D. M.; Kravis, L. D.; Cooley, A. J.; Chun, R.; MacEwen, E. G. Preclinical trial of doxorubicin entrapped in sterically stabilized liposomes in dogs with spontaneously arising malignant tumors. *Cancer Chemother. Pharmacol.* **1997**, *39*, 410−416.
(62) Gabizon, A. A. Pegylated liposomal doxorubicin: metamorphosis of an old drug into a new form of chemotherapy. *Cancer Invest.* **2001**, *19*, 424−436.
(63) Al-Jamal, K. T.; Al-Jamal, W. T.; Wang, J. T.; Rubio, N.; Buddle, J.; Gathercole, D.; Zloh, M.; Kostarelos, K. Cationic poly-L-lysine dendrimer complexes doxorubicin and delays tumor growth in vitro and in vivo. *ACS Nano* **2013**, *7*, 1905−1917.
(64) She, W.; Li, N.; Luo, K.; Guo, C.; Wang, G.; Geng, Y.; Gu, Z. Dendronized heparin−doxorubicin conjugate based nanoparticle as pH-responsive drug delivery system for cancer therapy. *Biomaterials* **2013**, *34*, 2252−2264.
(65) Graeser, R.; Esser, N.; Unger, H.; Fichtner, I.; Zhu, A.; Unger, C.; Kratz, F. INNO-206, the (6-maleimidocaproyl hydrazone derivative of doxorubicin), shows superior antitumor efficacy compared to doxorubicin in different tumor xenograft models and in an orthotopic pancreas carcinoma model. *Invest. New Drugs* **2010**, *28*, 14−19.
(66) Kratz, F.; Elsadek, B. Clinical impact of serum proteins on drug delivery. *J. Controlled Release* **2012**, *161*, 429−445.
(67) van der Vusse, G. J. Albumin as fatty acid transporter. *Drug Metab. Pharmacokinet.* **2009**, *24*, 300−307.
(68) Fujiwara, S.; Amisaki, T. Fatty acid binding to serum albumin: Molecular simulation approaches. *Biochim. Biophys. Acta* **2013**, *1830*, 5427−5434.

(69) Lim, S. I.; Mizuta, Y.; Takasu, A.; Hahn, Y. S.; Kim, Y. H.; Kwon, I. Site-specific fatty acid-conjugation to prolong protein half-life in vivo. *J. Controlled Release* **2013**, *170*, 219−225.
(70) Sparreboom, A.; Wolff, A. C.; Verweij, J.; Zabelina, Y.; van Zomeren, D. M.; McIntire, G. L.; Swindell, C. S.; Donehower, R. C.; Baker, S. D. Disposition of docosahexaenoic acid-paclitaxel, a novel taxane, in blood: In vitro and clinical pharmacokinetic studies. *Clin. Cancer Res.* **2003**, *9*, 151−159.
(71) Bradley, M. O.; Swindell, C. S.; Anthony, F. H.; Witman, P. A.; Devanesan, P.; Webb, N. L.; Baker, S. D.; Wolff, A. C.; Donehower, R. C. Tumor targeting by conjugation of DHA to paclitaxel. *J. Controlled Release* **2001**, *74*, 233−236.
(72) Homsi, J.; Bedikian, A. Y.; Papadopoulos, N. E.; Kim, K. B.; Hwu, W. J.; Mahoney, S. L.; Hwu, P. Phase 2 open-label study of weekly docosahexaenoic acid-paclitaxel in patients with metastatic uveal melanoma. *Melanoma Res.* **2010**, *20*, 507−510.
(73) Fracasso, P. M.; Picus, J.; Wildi, J. D.; Goodner, S. A.; Creekmore, A. N.; Gao, F.; Govindan, R.; Ellis, M. J.; Tan, B. R.; Linette, G. P.; Fu, C. J.; Pentikis, H. S.; Zumbrun, S. C.; Egorin, M. J.; Bellet, R. E. Phase 1 and pharmacokinetic study of weekly docosahexaenoic acid-paclitaxel, taxoprexin, in resistant solid tumor malignancies. *Cancer Chemother. Pharmacol.* **2009**, *63*, 451−458.